

Beyond the random phase approximation: Stimulated Brillouin backscatter for finite laser coherence times

Alexander O. Korotkevich,^{1,2} Pavel M. Lushnikov,^{1,*} and Harvey A. Rose³

¹*Department of Mathematics and Statistics, University of New Mexico, Albuquerque, NM 87131, USA*

²*Landau Institute for Theoretical Physics, 2 Kosygin Str., Moscow, 119334, Russia*

³*New Mexico Consortium, Los Alamos, New Mexico 87544, USA*

(Dated: August 26, 2021)

We develop a statistical theory of stimulated Brillouin backscatter (BSBS) of a spatially and temporally partially incoherent laser beam for laser fusion relevant plasma. We find a new collective regime of BSBS (CBSBS) with intensity threshold controlled by diffraction, an insensitive function of the laser coherence time, T_c , once light travel time during T_c exceeds a laser speckle length. The BSBS spatial gain rate is approximately the sum of that due to CBSBS, and a part which is independent of diffraction and varies linearly with T_c . We find that the bandwidth of KrF-laser-based fusion systems would be large enough to allow additional suppression of BSBS.

PACS numbers: 52.38.-r 52.38.Bv

I. INTRODUCTION

Inertial confinement fusion (ICF) experiments require propagation of intense laser light through underdense plasma subject to laser-plasma instabilities which can be deleterious for achievement of thermonuclear target ignition because they can cause the loss of target symmetry, energy and hot electron production [1]. Among laser-plasma instabilities, backward stimulated Brillouin scatter (BSBS) has long been considered a serious danger because the damping threshold of BSBS of coherent laser beams is typically several orders of magnitude less than the required laser intensity $\sim 10^{15}$ W/cm² for ICF. BSBS may result in laser energy retracing its path to the laser optical system, possibly damaging laser components [1, 2]. Recent experiments for a first time achieved conditions of fusion plasma and indeed demonstrated that large levels of BSBS (up to tens percent of reflectivity) are possible [3].

Theory of laser-plasma interaction instabilities is well developed for coherent laser beam [4]. However, ICF laser beams are not coherent because temporal and spatial beam smoothing techniques are currently used to produce laser beams with short enough correlation time, T_c , and lengths to suppress self-focusing [1, 2, 4]. The laser intensity forms a speckle field - a random in space distribution of intensity with transverse correlation length $l_c \simeq F\lambda_0$ and longitudinal correlation length (speckle length) $L_{speckle} \simeq 7F^2\lambda_0$, where F is the optic f -number and $\lambda_0 = 2\pi/k_0$ is the wavelength (see e.g. [5, 6]). There is a long history of study of amplification in random media (see e.g. [7, 8] and references there in). For small laser beam correlation time T_c , the spatial instability increment is given by a Random Phase Approximation (RPA). Beam smoothing for ICF typically has T_c much

above the regime of RPA applicability. There are few examples in which implications of laser beam spatial and temporal incoherence have been analyzed for such larger T_c . One exception is forward stimulated Brillouin scattering (FSBS). We have obtained in Refs. [9, 10] the FSBS dispersion relation for laser beam which has the correlation time T_c too large for RPA relevance, but still small enough to suppress single laser speckle instabilities [11]. We verified our theory of this ‘‘collective’’ FSBS instability regime with 3D simulations. Similar simulation results had been previously observed [25].

This naturally leads one to consider the possibility of a collective regime for BSBS (CBSBS). We present 2D and 3D simulation results as evidence for such a regime, and find agreement with a simple theory that above CBSBS threshold, the spatial increment for backscatter amplitude κ_i , is well approximated by the sum of two contributions. The first contribution is RPA-like $\propto T_c$ without intensity threshold (we neglect light wave damping). The second contribution has a threshold in laser intensity. That threshold is in parameter range of ICF hohlraum plasmas such as at the National Ignition Facility (NIF) [1] and the Omega laser facility (OMEGA) [13] experiments. The existence of threshold was first predicted in Ref. [12] in the limit $cT_c \gg L_{speckle}$, where c is the speed of flight [14]. The second contribution is collective-like because it neglects speckle contributions and is only weakly dependent on T_c . CBSBS threshold is applicable for strong and weak acoustic damping coefficient ν_{ia} . The theory also demonstrates a good quantitative prediction of the instability increment for small $\nu_{ia} \sim 0.01$ which is relevant for gold plasma near the wall of hohlraum in NIF and OMEGA experiments [1, 13].

The paper is organized as follows. In Section II we introduce the basic equations of BSBS for laser-plasma interaction and the stochastic boundary conditions which correspond to the partial incoherence of laser beam. In Section III we analyze the linearized BSBS equations and find the dispersion relations. In Section IV the convective versus absolute instabilities are analyzed from the

*Electronic address: plushnik@math.unm.edu

dispersion relations. Section V describes the details of the performed stochastic simulations of the full linearized equations. In section VI the conditions of applicability of the dispersion relation are discussed as well as the estimates for typical ICF experimental conditions are given. In Section VII the main results of the paper are discussed.

II. BASIC EQUATIONS

Assume that laser beam propagates in plasma with frequency ω_0 along z . The electric field \mathcal{E} is given by

$$\mathcal{E} = (1/2)e^{-i\omega_0 t} \left[E e^{ik_0 z} + B e^{-ik_0 z - i\Delta\omega t} \right] + c.c., \quad (1)$$

where $E(\mathbf{r}, z, t)$ is the envelope of laser beam and $B(\mathbf{r}, z, t)$ is the envelope of backscattered wave, $\mathbf{r} = (x, y)$, and c.c. means complex conjugated terms. Frequency shift $\Delta\omega = -2k_0 c_s$ is determined by coupling of E and B through ion-acoustic wave of phase speed c_s and wavevector $2k_0$ with plasma density fluctuation δn_e given by $\frac{\delta n_e}{n_e} = \frac{1}{2}\sigma e^{2ik_0 z + i\Delta\omega t} + c.c.$, where $\sigma(\mathbf{r}, z, t)$ is the slow envelope (slow provided $\Delta\omega T_c \gg 1$) and n_e is the average electron density, assumed small compared to the critical electron density n_c . We consider a slab model of plasma (plasma parameters are uniform). The coupling of E and B to plasma density fluctuations gives

$$R_{EE}^{-1} E \equiv \left[i \left(c^{-1} \partial_t + \partial_z \right) + \frac{1}{2k_0} \nabla^2 \right] E = \frac{k_0}{4} \frac{n_e}{n_c} \sigma B, \quad (2)$$

$$R_{BB}^{-1} B \equiv \left[i \left(c^{-1} \partial_t - \partial_z \right) + \frac{1}{2k_0} \nabla^2 \right] B = \frac{k_0}{4} \frac{n_e}{n_c} \sigma^* E, \quad (3)$$

$\nabla = (\partial_x, \partial_y)$, and σ is described by the acoustic wave equation coupled to the ponderomotive force $\propto \mathcal{E}^2$ which results in the envelope equation

$$R_{\sigma\sigma}^{-1} \sigma^* \equiv \left[i \left(c_s^{-1} \partial_t + 2\nu_{ia} k_0 + \partial_z \right) - (4k_0)^{-1} \nabla^2 \right] \sigma^* = -2k_0 E^* B. \quad (4)$$

Here we neglected terms $\propto |E|^2$, $|B|^2$ in the right-hand side (r.h.s.) which are responsible for self-focusing effects, ν_L is the Landau damping of ion-acoustic wave and $\nu_{ia} = \nu_L / 2k_0 c_s$ is the scaled acoustic Landau damping coefficient. E and B are in thermal units (see e.g. [9]) defined so that if we add self-focusing term $I = |E|^2$ in r.h.s. of Eq. (4) then in equilibrium, with uniform E , the standard $\delta n_e / n_e = \exp(-I) - 1$ is recovered.

We use a simple model of induced spacial incoherence beam smoothing [20] which defines stochastic boundary conditions at $z = 0$ for spatial Fourier transform (over \mathbf{r}) components $\hat{E}(\mathbf{k})$, of laser beam amplitude [9]:

$$\begin{aligned} \hat{E}(\mathbf{k}, z = 0, t) &= |E_{\mathbf{k}}| \exp[i\phi_{\mathbf{k}}(t)], \\ \langle \exp i[\phi_{\mathbf{k}}(t) - \phi_{\mathbf{k}'}(t')] \rangle &= \delta_{\mathbf{k}\mathbf{k}'} \exp(-|t - t'|/T_c), \end{aligned} \quad (5)$$

where

$$|E_{\mathbf{k}}| = \text{const}, \quad k < k_m; \quad E_{\mathbf{k}} = 0, \quad k > k_m, \quad (6)$$

is chosen as the idealized ‘‘top hat’’ model of NIF optics [21]. Here $\langle \dots \rangle$ means the averaging over the ensemble of stochastic realizations of boundary conditions, $k_m \simeq k_0 / (2F)$ is the top hat width and the average intensity, $\langle I \rangle \equiv \langle |E|^2 \rangle = I$ determines the constant.

III. LINEARIZED EQUATIONS AND DISPERSION RELATIONS

In linear approximation, assuming $|B| \ll |E|$ so that only the laser beam is BSBS unstable, we neglect right hand side (r.h.s.) of Eq. (2). The resulting linear equation with boundary condition (5) has the exact solution as decomposition of E into Fourier series,

$$E(\mathbf{r}, z, t) = \sum_j E_{\mathbf{k}_j},$$

$$E_{\mathbf{k}_j} = |E_{\mathbf{k}_j}| \exp \left[i \left(\phi_{\mathbf{k}_j}(t - z/c) + \mathbf{k}_j \cdot \mathbf{r} - \mathbf{k}_j^2 z / 2k_0 \right) \right]. \quad (7)$$

Figures 1 show the increment κ_i of the spatial growth of backscattered light intensity $\langle |B|^2 \rangle \propto e^{-2\kappa_i z}$ as a function of the rescaled correlation time \tilde{T}_c obtained from the numerical solution of the stochastic linear equations (3)-(7) (details of numerical simulations are provided in Section V), the scaled damping rate μ and the scaled laser intensity \tilde{I} . These scaling quantities are defined as

$$\tilde{T}_c \equiv T_c k_0 c_s / 4F^2, \quad \mu \equiv 2\nu_{ia} k_0^2 / k_m^2, \quad \tilde{I} \equiv \frac{4F^2}{\nu_{ia}} \frac{n_e}{n_c} I. \quad (8)$$

Here \tilde{T}_c has the meaning of the correlation time T_c in units of the acoustic transit time along speckle. (Note that definition of \tilde{T}_c is different by a factor $1/2F$ from the definition used for FSBS [9, 10], where units of the transverse acoustic transit time through speckle were used.) We use dimensionless units with $k_0/k_m^2 = 4F^2/k_0$ as the unit in z direction, and $k_0/k_m^2 c_s$ is the time unit. $\langle \dots \rangle$ means averaging over the statistics of laser beam fluctuations (5). μ is the damping rate in units of the inverse acoustic propagation time along a speckle. (See also Figure 4 below for illustration of intensity normalization in comparison with physical units.)

We relate κ_i to the instability increments for $\langle B \rangle$ and $\langle \sigma^* \rangle$ (we designate them κ_B and κ_σ , respectively). In general, growth rates of mean amplitudes give a lower bound to κ_i . However, according to Figure 2, σ is almost coherent on a time scale T_c justifying the use of mean values of amplitudes.

First we look for the expression for κ_σ . Eq. (3) is linear in B and E implying that B can be decomposed into $B = \sum_j B_{\mathbf{k}_j}$ with

$$R_{BB}^{-1} B_{\mathbf{k}_j} = \frac{k_0}{4} \frac{n_e}{n_c} \sigma^* E_{\mathbf{k}_j}. \quad (9)$$

Approximating r.h.s. of (4) as $E^* B \simeq \sum_j E_{\mathbf{k}_j}^* B_{\mathbf{k}_j}$ gives

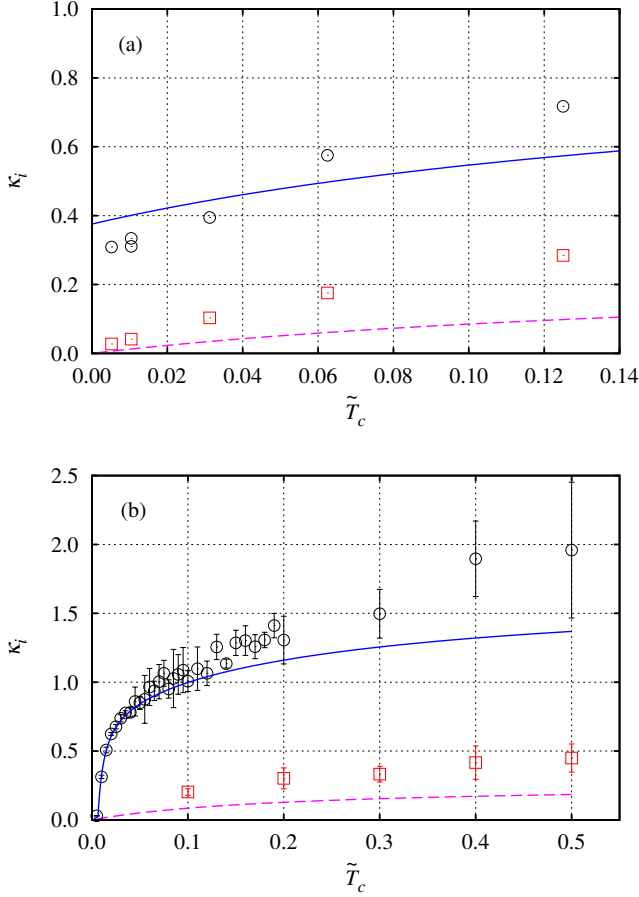


FIG. 1: Spatial increment κ_i of CBSBS obtained from stochastic simulations of (3)-(7) compared with the sum of increments $\kappa_B + \kappa_\sigma$ (obtained by solving (16) and (21)). The scaled damping rate $\mu = 5.12$ is used (e.g. it corresponds to $\nu_{ia} = 0.01$, $F = 8$). (a) 3D simulations with $c_s/c = 0$, $\tilde{I} = 2$ (circles) and $\tilde{I} = 1$ (squares). The scaled dimensionless laser intensity \tilde{I} , μ and the scaled correlation time \tilde{T}_c are defined in (8). Solid and dashed lines show $\kappa_B + \kappa_\sigma$ for $\tilde{I} = 2$ and $\tilde{I} = 1$, respectively. If $\kappa_\sigma < 0$ then $\kappa_B + \kappa_\sigma$ is replaced by κ_B . (b) 2D simulations with the modified boundary conditions, $c/c_c = 500$, $\tilde{I} = 3$ (circles) and $\tilde{I} = 1$ (squares). Error bars are also shown. Solid and dashed lines show $\kappa_B + \kappa_\sigma$ for $\tilde{I} = 3$ and $\tilde{I} = 1$, respectively, for both (a) and (b). The details of simulation method are provided in Section V.

$$R_{\sigma\sigma}^{-1}\sigma^* = -2k_0 \sum_j E_{\mathbf{k}_j}^* B_{\mathbf{k}_j}, \quad (10)$$

which means that we neglect off-diagonal terms $E_{\mathbf{k}_j}^* B_{\mathbf{k}_{j'}}$, $j \neq j'$. Since speckles of laser field arise from interference of different Fourier modes, $j \neq j'$, we associate the off-diagonal terms with speckle contribution to BSBS [5, 15, 22]. Neglecting off-diagonal terms requires that during time T_c light travels much further than a speckle length, $L_{\text{speckle}} \ll cT_c$ and that $T_c \ll t_{\text{sat}}$, where t_{sat} is the characteristic time scale at which BSBS con-

vective gain saturates at each speckle [18].

Eqs. (9) and (10) result in

$$R_{\sigma\sigma}^{-1}\langle\sigma^*\rangle = -(k_0^2/2)(n_e/n_c)\langle\sum_j E_{\mathbf{k}_j}^* R_{BB}\sigma^* E_{\mathbf{k}_j}\rangle \quad (11)$$

with the Fourier transformed R_{BB} given by

$$\hat{R}_{BB}(\mathbf{k}, z, t) = -ic\delta(z + ct) \exp[i\frac{k^2}{2k_0}z]\Theta(-z), \quad (12)$$

where $\Theta(z)$ is the Heaviside step function.

We assume that σ^* is slow in comparison with $E_{\mathbf{k}_j}$ (consistent with Figure 2) which allows to approximate fluctuating terms in r.h.s. of (11) as $\langle E_{\mathbf{k}_j}^* \sigma^* E_{\mathbf{k}_j} \rangle \simeq \langle\sigma^*\rangle\langle E_{\mathbf{k}_j}^* E_{\mathbf{k}_j} \rangle$ which has the same form as the Bourret approximation [8] and provides the closed expression for $\langle\sigma^*\rangle$ as follows

$$R_{\sigma\sigma}^{-1}\langle\sigma^*(\mathbf{r}, z, t)\rangle = -(k_0^2/2)(n_e/n_c) \int \int \int d\mathbf{r}' dz' dt' \\ \times R_{BB}(\mathbf{r} - \mathbf{r}', z - z', t - t') C^*(\mathbf{r} - \mathbf{r}', z - z', t - t') \\ \times \langle\sigma^*(\mathbf{r}', z', t')\rangle, \quad (13)$$

where the kernel of the response function $R_{BB}(\mathbf{x}, z, t)$ is the inverse Fourier transform of (12) and the laser beam correlation function C is given by

$$C(\mathbf{r} - \mathbf{r}', z - z', t - t') \equiv \langle E(\mathbf{r}, z, t) E^*(\mathbf{r}', z', t') \rangle \\ = \sum_j |E_{\mathbf{k}_j}|^2 \exp\left[i\mathbf{k}_j \cdot (\mathbf{r} - \mathbf{r}') - i\frac{\mathbf{k}_j^2}{2k_0}(z - z') - |t - t' - (z - z')/c|/T_c\right] \quad (14)$$

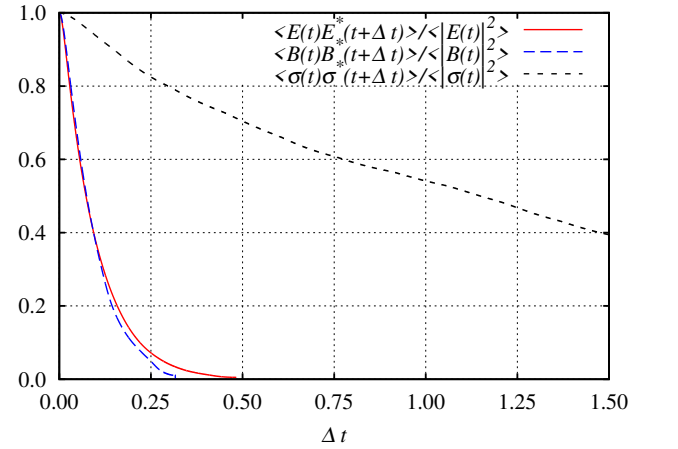


FIG. 2: Normalized autocorrelation functions vs. a dimensionless time shift Δt for E , B and σ : $\langle E(\mathbf{r}, z, t) E^*(\mathbf{r}, z, t + \Delta t) \rangle$, $\langle B(\mathbf{r}, z, t) B^*(\mathbf{r}, z, t + \Delta t) \rangle$ and $\langle \sigma(\mathbf{r}, z, t) \sigma^*(\mathbf{r}, z, t + \Delta t) \rangle$ with $\tilde{I} = 3$, $\tilde{T}_c = 0.1$ and $\mu = 5.12$ from stochastic simulations of (3)-(7). It is seen that B is correlated at the same time \tilde{T}_c as E while ρ is correlated at much larger times.

for the top hat model (5),(6) and (7).

We look for solution of (13) in exponential form $\langle \sigma^* \rangle \propto e^{i(\kappa z + \mathbf{k} \cdot \mathbf{r} - \omega t)}$, then the exponential time dependence of (14) allows to carry all integrations in (12) and (13) explicitly to arrive at the following dispersion relation in dimensionless units

$$\begin{aligned} & -i\omega + \mu + i\kappa - (i/4)k^2 \\ & = 8iF^4 \frac{n_e}{n_c} \sum_{j=1}^N \frac{|E_{\mathbf{k}_j}|^2}{\omega \frac{c_s}{c} + \kappa - k_j^2 - \frac{k^2}{2} - \mathbf{k}_j \cdot \mathbf{k} + 2i \frac{c_s}{c} \frac{1}{T_c}}, \end{aligned} \quad (15)$$

where vectors \mathbf{k}_j span top hat (5),(6), and $I = \sum_j |E_{\mathbf{k}_j}|^2$.

In the continuous limit $N \rightarrow \infty$, sum in (15) is replaced by integral, giving for the most unstable mode $\mathbf{k} = 0$:

$$\begin{aligned} \Delta_\sigma(\omega, \kappa) &= -i\omega + \mu + i\kappa \\ &+ i \frac{\mu}{4} \tilde{I} \ln \frac{1 - \kappa - \omega \frac{c_s}{c} - 2i \frac{c_s}{c} \frac{1}{T_c}}{-\kappa - \omega \frac{c_s}{c} - 2i \frac{c_s}{c} \frac{1}{T_c}} = 0, \end{aligned} \quad (16)$$

which supports the convective instability with the increment $\kappa_\sigma \equiv \text{Im}(\kappa) > 0$ only for $\tilde{I} > \tilde{I}_{convthresh}$, where $\tilde{I}_{convthresh}$ is the convective CBSBS threshold given by

$$\tilde{I}_{convthresh} = \frac{4}{\pi} \left(1 - \frac{8c_s}{\pi c \tilde{I}_c} \right)^{-1}. \quad (17)$$

In the limit $c/c_s \rightarrow \infty$, the increment κ_σ is independent of \tilde{I}_c which suggests that we refer to it as the collective instability branch. For finite but small $c_s/c \ll 1$ and $\tilde{I} > \tilde{I}_{convthresh}$ there is sharp transition of κ_σ as a function of \tilde{I}_c from 0 for $\tilde{I}_c = 0$ to \tilde{I}_c -independent value of κ_σ . That value can be obtained analytically from (16) for I just above the threshold as follows: $\kappa_\sigma = \mu(\pi/4 - 2\tilde{I}_c^{-1}c_s/c)(\tilde{I} - \tilde{I}_{convthresh})/(\mu\tilde{I} - 1)$ [24].

The increment κ_B is obtained in a similar way by statistical averaging of equation (3) for $\langle B \rangle$ which gives

$$R_{BB}^{-1} \langle B \rangle = -(k_0^2/2)(n_e/n_c) \langle ER_{\sigma\sigma} E^* B \rangle \quad (18)$$

with the Fourier transformed response function

$$\hat{R}_{\sigma\sigma}(\mathbf{k}, z, t) = -ic_s \delta(z - c_s t) \exp \left[\left(i \frac{k^2}{4k_0} - 2\nu_{ia} k_0 \right) z \right] \Theta(z) \quad (19)$$

Then the Bourret approximation (18) results in the following closed expression for $\langle B \rangle$:

$$\begin{aligned} R_{BB}^{-1} \langle B(\mathbf{r}, z, t) \rangle &= -(k_0^2/2)(n_e/n_c) \int \int \int d\mathbf{r}' dz' dt' \\ &\times R_{\sigma\sigma}(\mathbf{r} - \mathbf{r}', z - z', t - t') C^*(\mathbf{r} - \mathbf{r}', z - z', t - t') \\ &\times \langle B(\mathbf{r}', z', t') \rangle, \end{aligned} \quad (20)$$

where the kernel of the response function $R_{\sigma\sigma}(\mathbf{x}, z, t)$ is the inverse Fourier transform of (19) and C is given by (14).

We look for solution of (13) in exponential form $\langle B \rangle \propto e^{i(\kappa z + \mathbf{k} \cdot \mathbf{r} - \omega t)}$, then the exponential time dependence of

(14) allows to carry all integrations in (19) and (20) explicitly to arrive at the following dispersion relation in dimensionless units

$$\begin{aligned} \Delta_B(\omega, \kappa) &= i\omega \frac{c_s}{c} + i\kappa \\ &+ i \frac{\mu}{4} \tilde{I} \frac{1}{\kappa - \omega - i\mu - i \frac{1}{T_c}} = 0. \end{aligned} \quad (21)$$

Here we neglected the contribution to $\kappa_B \equiv \text{Im}(\kappa)$ from diffraction and used the condition $c_s/c \ll 1$. Equation (21) does not have a convective threshold (provided we neglect here light wave damping) while κ_B has near-linear dependence on \tilde{I}_c : $\kappa_B \simeq \mu \tilde{I} \tilde{I}_c / 4$ for $\tilde{I}_c < 1/\mu$ which is typical for RPA results. It suggests that we refer κ_B as the RPA-like branch of instability.

Solving the equations (16) and (21) numerically for κ allows to find κ_σ and κ_B , respectively, for given ω . We choose $\omega = 0.5$ in (16) and $\omega = 0$ in (21) to maximize κ_σ and κ_B , respectively. Figures 1a and 1b show that the analytical expression $\kappa_B + \kappa_\sigma$ is a reasonably good approximation for numerical value of κ_i above the convective threshold (17) for $\tilde{I}_c \lesssim 0.1$ which is the main result of this paper. Below this threshold analytical and numerical results are only in qualitative agreement and we replace $\kappa_B + \kappa_\sigma$ by κ_B because $\kappa_\sigma < 0$ in that case.

The qualitative explanation why $\kappa_B + \kappa_\sigma$ is a surprisingly good approximation to κ_i is based on the following argument. First imagine that B propagates linearly and not coupled to the fluctuations of σ^* , so its source is $\sigma^* E \rightarrow \langle \sigma^* \rangle E$ in r.h.s of (3). If $\langle \sigma^* \rangle \propto e^{\kappa_\sigma z}$ grows slowly with z (i.e. if $\langle \sigma^* \rangle$ changes a little over the speckle length $L_{speckle}$ and time T_c), then so will $\langle |B|^2 \rangle$ at the rate $2\kappa_\sigma$. But if the total linear response R_{BB}^{tot} (R_{BB}^{tot} is the renormalization of bare response R_{BB} due to the coupling in r.h.s of (3)) is unstable then its growth rate gets added to κ_σ in the determination of $\langle |B|^2 \rangle$ since in all theories which allow factorization of 4-point correlation function into product of 2-point correlation functions, $\langle B(1)B^*(2) \rangle = R_{BB}^{tot}(1, 1')S(1', 2')R_{BB}^{tot*}(2', 2)$. Here $S(1, 2) \equiv \langle \sigma^*(1)\sigma(2) \rangle \langle E(1)E^*(2) \rangle \simeq \langle \sigma^*(1) \rangle \langle \sigma(2) \rangle \langle E(1)E^*(2) \rangle$ and “1”, “2” etc. mean a set of all spatial and temporal arguments.

IV. CONVECTIVE INSTABILITY VERSUS ABSOLUTE INSTABILITY

In this Section we show that the dispersion relations (16) and (21) predict absolute instability for large intensities. We first consider the dispersion relation (16) which has branch cut in the complex κ -plane connecting two branch points $\kappa_1 = 1 - \omega \frac{c_s}{c} - 2i \frac{c_s}{c} \frac{1}{T_c}$ and $\kappa_2 = -\omega \frac{c_s}{c} - 2i \frac{c_s}{c} \frac{1}{T_c}$.

Absolute instability occurs if the contour $\text{Im}(\omega) = \text{const}$ in the complex ω -plane cannot be moved down to real ω axis because of pinching of two solutions of (16) in the complex κ -plane [16],[17]. To describe instability one of these solutions must cross the real axis in κ -plane as

the contour $Im(\omega) = const$ is moving down. The pinch occurs provided

$$\frac{\partial \Delta_\sigma(\omega, \kappa)}{\partial \kappa} = 0. \quad (22)$$

The pinch condition (22) together with the requirement of crossing the real axis in κ -plane result in

$$\kappa = \frac{1}{2} + \frac{1}{2}i\sqrt{\mu\tilde{I} - 1} - \frac{c_s}{c}\omega - \frac{c_s}{c}\frac{2i}{\tilde{T}_c}. \quad (23)$$

Taking (23) together with $\Delta_\sigma(\omega, \kappa) = 0$ from (16) at the absolute instability threshold $Im(\omega) = 0$ gives the transcendental expression

$$\begin{aligned} \mu - \frac{1}{2}(\mu\tilde{I}_{absthresh} - 1)^{1/2} + \frac{c_s}{c}\frac{2}{\tilde{T}_c} \\ - \frac{1}{2}\mu\tilde{I}_{absthresh} \arctan\left[(\mu\tilde{I}_{absthresh} - 1)^{-1/2}\right] = 0 \end{aligned} \quad (24)$$

for the absolute instability threshold intensity $\tilde{I}_{absthresh}$. Assuming $\mu\tilde{I}_{absthresh} \gg 1$ we obtain from (24) the explicit expression for the CBSBS absolute instability threshold

$$\tilde{I}_{absthresh} = \mu + 3\mu^{-1} + O(\mu^{-3}) + O(\tilde{T}_c^{-1}c_s/c). \quad (25)$$

The absolute instability threshold for the second RPA-like branch (21) is obtained similarly with the pinch condition $\frac{\partial \Delta_B(\omega, \kappa)}{\partial \kappa} = 0$. It gives the absolute instability threshold for RPA-like branch of instability

$$\tilde{I}_{absthresh, B} = \mu \left(1 + \frac{1}{\mu\tilde{T}_c}\right)^2. \quad (26)$$

For $\tilde{T}_c \lesssim 1$, the threshold (25) is lower than (26) thus (26) can be ignored.

For $\mu \gg 1$ the absolute threshold (25) reduces to the coherent absolute BSBS instability threshold

$$\tilde{I}_{absthreshcoherent} = \mu. \quad (27)$$

For typical experimental condition $\mu \gtrsim 5$. Then the absolute instability threshold (25) is significantly above the convective instability threshold (17). Thus in simulations described below we emphasize the convective regime and assume \tilde{I} to be below the absolute threshold.

V. NUMERICAL SIMULATIONS

We performed two types of simulations. First type is 3+1D simulations (three spatial coordinates \mathbf{r} , z and t) of Eqs. (3), (4) and (7) with the boundary and initial conditions (5),(6) in the limit $c \rightarrow \infty$ (i.e., setting $c^{-1} = 0$ in (3) and (4)). It implies that the phases $\phi_{\mathbf{k}_j}(t - z/c)$ in (7) become only t -dependent, $\phi_{\mathbf{k}_j}(t)$. That formal limit $c \rightarrow \infty$, is consistent provided $c\tilde{T}_c \gg L_{speckle}$. Then in

the linear instability regime, the laser field, E , at any time may be obtained by propagation from $z = 0$ while the scattered light field, B is obtained by backward propagation from $z = L_z$. Time scales are now set by the minimum of T_c and the acoustic time scale for the density σ^* . We performed numerical simulation of B and σ^* via a split-step (operator splitting) method. E advances only due to diffraction and is determined exactly by (7). For given σ^* , B is first advanced due to diffraction in transverse Fourier space, and then the source term (r.h.s. of (3) which is $\propto \sigma^*E$) is added for all $\mathbf{r} = (x, y)$. The density σ^* is evolved in the strong damping approximation in which the d/dz term is omitted from equation (4). In the regimes of interest, in particular near the collective threshold (17) regime, the dimensionless damping coefficient in (4) increases with acoustic Landau damping coefficient, and even for its physically smallest value of 0.01, the scaled damping μ is approximately 5 while d/dz is either $\simeq \kappa_i$ or $1/10$ (an inverse speckle length). So given E and B , σ^* may be advanced in time at each z , for each transverse Fourier mode, or since the transverse Laplacian term is estimated as unity in magnitude (base on the speckle width estimate of $F\lambda_0$), σ^* may be approximately advanced at each spatial lattice point.

Second type is 2+1D simulations (two spatial coordinates x , z and t) of Eqs. (3),(4) and(7) with finite value $c_s/c = 1/500$ (the typical value for the experiment) and modified top-hat boundary condition

$$|E_{\mathbf{k}}| = k^{1/2} const, \quad k < k_m; \quad E_{\mathbf{k}} = 0, \quad k > k_m, \quad (28)$$

chosen to mimic the extra factor k in the integral over transverse direction of the full 3+1D problem. That modified top hat choice ensures that the linearized equations of that 2+1D problem give exactly the same analytical solutions (16) and (21) as for the full 3+1D problem. We used again the split step method by integrating along the characteristics of ρ and B and solving for the diffraction by Fourier transform in the transverse coordinate x .

We run simulations in the box $0 < z < L_z$. For both types of simulations the boundary conditions for B were set at $z = L_z$. We take these boundary conditions as the Fourier modes of $B(\mathbf{r}, z = L_z, t)$ in \mathbf{r} with random time-independent phases. These modes correspond to the random seed from the thermal fluctuations. The boundary conditions for ρ were set to be zero. As the time progress from the beginning of each simulation, both $|\rho|$ and $|B|^2$ grow until reaching the statistical steady state if the \tilde{I} is below the threshold of absolute instability (25). Figure 3 shows a typical time dependence of $\langle |B|^2 \rangle_x$, where $\langle \dots \rangle_x$ means averaging over the transverse coordinate x . Because we solve linear equations (3) and (4), the maximum value of $\langle |B|^2 \rangle_x$ grows if we increase L_z as well as the boundary condition $B(\mathbf{r}, z = L_z, t)$ is defined up to the multiplication by the arbitrary constant. z -dependence of $\langle |B|^2 \rangle_x$ in the statistical steady state follows the exponential law $\langle |B|^2 \rangle_x \propto e^{-2\kappa_i z}$ well inside the interval $0 < z < L_z$. Near the boundaries $z = 0$ and $z = L_z$

there are short transition layers before solution settles at $e^{-2\kappa_i z}$ law inside that interval. The particular form of the boundary conditions for B and ρ affect only these transition layers while $e^{-2\kappa_i z}$ law is insensitive to them.

To recover κ_i with high precision we performed simulations for long time after reaching statistical steady state and average $\langle |B|^2 \rangle_x$ over that time at each z (i.e. we assumed ergodicity). E.g. for $\tilde{T}_c = 0.1$ (the time the laser light travels along $\simeq 5$ laser speckles) we use 256 transverse Fourier modes and discrete steps $\Delta z = 0.15$ in dimensionless units with the typical length of the system $L_z = 50$ ($\simeq 5$ speckle lengths) and a time step $\Delta t = \Delta z c_s / c$. For this particular set of parameters it implies $\Delta t = 3 \cdot 10^{-4}$. For simulation we typically wait $\sim 10^5 - 10^6$ time steps to achieve a robust statistical steady state and then average over another $\sim 10^5 - 10^6$ time steps (together with averaging over the transverse coordinates) to find κ_i with high precision. Figures 1a and 1b show κ_i extracted from 3 + 1D and 2 + 1D simulations, respectively.

For the practical purposes it is also interesting to estimate the time t_{ini} at which the initial thermal fluctuations of $|B|^2$ are amplified by $\sim e^{20}$ to reach the comparable intensity with the laser pump. We obtained from simulations that $t_{ini} \sim 0.7$ for $L_z \simeq$ two laser speckles (relevant for gold plasma in ICF experiments and corresponds to $L_z \simeq 22$ in dimensionless units), $\tilde{I} = 3$ and $\tilde{T}_c = 0.1$. In dimensional units for NIF conditions $t_{ini} \sim 20$ ps which is well below hydrodynamic time (several hundreds of ps).

Figure 2 shows normalized autocorrelation functions $\langle E(\mathbf{r}, z, t)E^*(\mathbf{r}, z, t + \Delta t) \rangle$, $\langle B(\mathbf{r}, z, t)B^*(\mathbf{r}, z, t + \Delta t) \rangle$ and $\langle \sigma(\mathbf{r}, z, t)\sigma^*(\mathbf{r}, z, t + \Delta t) \rangle$ for $\tilde{T}_c = 0.1$. It is seen that the

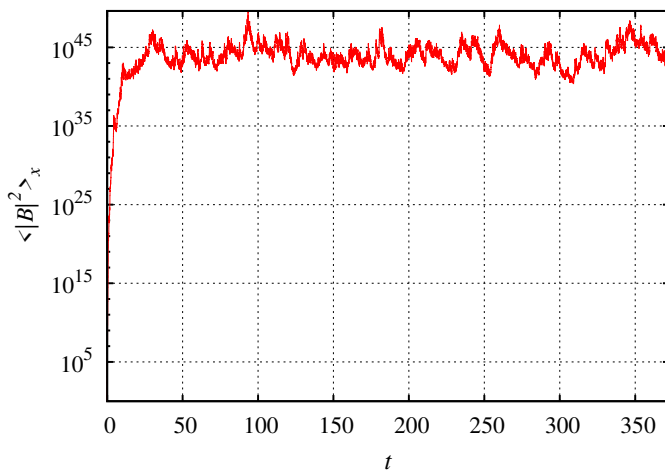


FIG. 3: The time dependence of $\langle |B|^2 \rangle_x$ for 3+1D simulation with $L_z = 50$, $\mu = 5.12$, $\tilde{T}_c = 0.1$ and $\tilde{I} = 3.0$. $\langle |B|^2 \rangle_x$ is shown at $z = 25$. It is seen that after the initial growth, $\langle |B|^2 \rangle_x$ settles at the statistical steady state with the large fluctuations around it. The boundary condition at $z = L_z$ is $\langle |B|^2 \rangle_x \sim 1$.

correlation times for E and B are similar while the correlation time for σ is much larger, the more so the smaller \tilde{T}_c . This justifies the use of the analytical approximations of the Section III.

VI. APPLICABILITY OF THE DISPERSION RELATION AND ESTIMATES FOR EXPERIMENT

The applicability conditions of the Bourret approximation used in derivation of (16) and (21) in the dimensionless units are

$$\Delta\omega_B \Delta\omega_\sigma \gg \gamma_0^2. \quad (29)$$

and $\Delta\omega_B \gg (c/c_s)|\kappa_B|$ as well as $\Delta\omega_\sigma \gg \mu$. Here γ_0 is the temporal growth rate of the spatially homogeneous solution given by $\gamma_0^2 = (1/4)(c/c_s)\mu\tilde{I}$. Also $\Delta\omega_\sigma = 1/\tilde{T}_c$ is the bandwidth for σ and $\Delta\omega_B$ is the effective bandwidth for B . $\Delta\omega_B$ is dominated by the diffraction in (3) giving in the dimensionless units $\Delta\omega_B = c/c_s$. Then (29) reduces to $\tilde{T}_c \ll 4/(\mu\tilde{I})$ and $|\kappa_B| \ll 1$. Together with the condition $\tilde{T}_c \gg L_{speckle}/c$ used in the derivation of (16) and assuming that $\tilde{I} \simeq \tilde{I}_{convthresh}$, it gives a double inequality $(7\pi/2)(c/c_s) \ll \tilde{T}_c \ll \pi/\mu$ which can be well satisfied for $\mu \simeq 5$, i.e. for $\nu_{ia} \simeq 0.01$ as in gold ICF plasma but not for $\mu \simeq 50$ as in low ionization number Z ICF plasma. Also $|\kappa_B| < 1$ implies that $\tilde{I} > \tilde{I}_{convthresh}$ because otherwise, below that threshold, $\kappa_B \sim -\mu$ which would contradict $|\kappa_B| < 1$. All these conditions are satisfied for $\tilde{T}_c \lesssim 1/4$ for the parameters of Figure 1 with $\tilde{I} = 2$ or $\tilde{I} = 3$ (solid lines in Figure 1) but not for $\tilde{I} = 1$ (dashed lines in Figure 1). Additionally, an estimate for $\tilde{T}_c \ll t_{sat}$ from the linear part of the theory of Ref. [18] results in the condition $\tilde{T}_c \ll 8\tilde{I}/\mu$ which is less restrictive than above conditions. These estimates are consistent with the observed agreement between $\kappa_i = \kappa_\sigma + \kappa_B$ and κ_i from simulations (filled circles in Figures 1) for \tilde{I} above the threshold (17). We conclude from Figures 1 that the applicability condition for the Bourret approximation is close to the domain of \tilde{T}_c values for which $\kappa_i = \kappa_\sigma + \kappa_B$.

For nominal NIF parameters [1, 10], $F = 8$, $n_e/n_c = 0.1$, $\lambda_0 = 351$ nm, $c_s = 6 \times 10^7$ cm s $^{-1}$ and electron plasma temperature $T_e \simeq 2.6$ keV (T_e was recently updated from the old standard value $T_e \simeq 5$ keV [23]), we obtain from (17) that $I_{convthresh} \simeq 1.1 \times 10^{14}$ W/cm 2 for gold plasma with $\nu_{ia} \simeq 0.01$ which is in the range of NIF single polarization intensities. Fig. 4 shows κ_i in the limit $c_s/c = 0$, $\tilde{T}_c \rightarrow 0$ from simulations, analytical result κ_σ ($\kappa_B = 0$ in that limit) and the instability increment of the coherent laser beam $\kappa_{coherent} = \mu/2 - (\mu^2 - \mu\tilde{I})^{1/2}/2$ (see e.g. [4]). It is seen that the coherent increment significantly overestimates numerical increment especially around $I_{convthresh}$. The convective increment κ_i has a significant dependence on \tilde{T}_c if we include the effect of finite $c/c_s = 500$ and finite \tilde{T}_c as in Fig. 1b. Cur-

rent NIF 3Å beam smoothing design has $T_c \simeq 4\text{ps}$ implying $\tilde{T} \simeq 0.15$. In that case Fig. 1b shows that there is a significant (about 5 fold) change in κ_i between $\tilde{I} = 1$ and $\tilde{I} = 3$. Similar estimate for KrF lasers ($\lambda_0 = 248\text{nm}$, $F = 8$, $T_c = 0.7\text{ps}$) gives $\tilde{T}_c = 0.04$ which results in a significant (40%) reduction of κ_i for $\tilde{I} = 3$ compare with above NIF estimate.

The BSBS threshold may be reduced by self-induced temporal incoherence (see e.g. [25]), which in its linear regime, includes collective FSBS (CFSBS) which reduces T_c and laser correlation lengths. For low Z plasma, the CBSBS and CFSBS thresholds are close while the latter may be lowered by adding higher Z dopant.

VII. CONCLUSION

In conclusion, we identified the collective threshold (17) of BSBS instability of partially incoherent laser beam for ICF relevant plasma. Above that threshold the CBSBS increment κ_i is well approximated by the sum of the collective-like increment κ_σ and RPA-like increment κ_B . That result is in agreement with the direct stochastic simulations of BSBS equations. Values of κ_σ

and κ_B are comparable above threshold while in a small neighborhood of threshold the value of κ_i changes quickly with changing either correlation time or laser intensity to pass through collective threshold. With further increase of laser intensity the absolute instability also develops above the threshold (25).

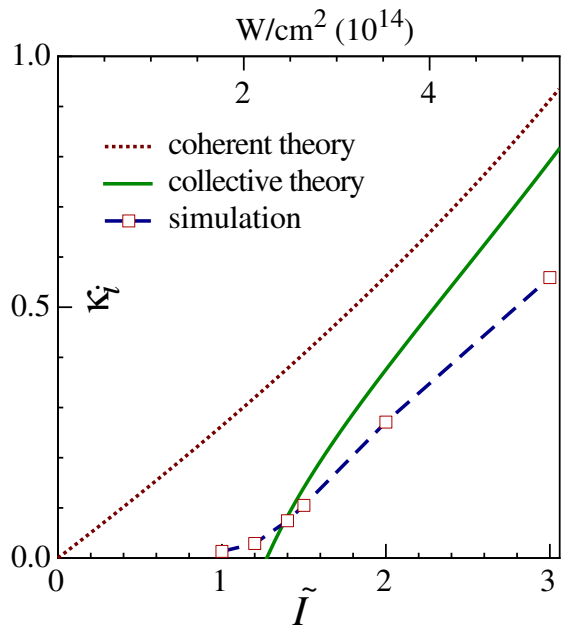


FIG. 4: κ_i vs. \tilde{I} for $\mu = 5.12$ obtained from $3 + 1D$ simulations (squares connected by dashed line, $c_s/c = 0$ and limit $\tilde{T}_c \rightarrow 0$ taken by extrapolation from $\tilde{T}_c \ll 1$), analytical result κ_σ (solid curve) and coherent laser beam increment $\kappa_{coherent}$ (dotted curve). The scaled dimensionless laser intensity \tilde{I} and damping rate μ in units of acoustic propagation time along a speckle are defined in (8). Upper grid corresponds to laser intensity in dimensional units $I_{physical} \propto T_e/\lambda_0^2$ for NIF parameters and gold plasma $T_e \simeq 5\text{keV}$, $F = 8$, $n_e/n_c = 0.1$, $\nu_{ia} = 0.01$, $\lambda_0 = 351\text{nm}$.

Acknowledgments

We acknowledge helpful discussions with R. Berger and N. Meezan. P.L. and H.R. were supported by the New Mexico Consortium and Department of Energy Award No. DE-SC0002238 as well as by the National Science Foundation under Grants No. PHY 1004118, and No. PHY 1004110. A.K. was partially supported by the Program “Fundamental problems of nonlinear dynamics” from the RAS Presidium and “Leading Scientific Schools of Russia” grant NSh-6170.2012.2.

-
- [1] J. D. Lindl, *et al.*, Phys. Plasmas **11**, 339 (2004).
- [2] N. B. Meezan, *et al.*, Phys. Plasmas **17**, 056304 (2010).
- [3] S. H. Glenzer *et al.*, Nature Phys., **3**, 716 (2007); D. H. Froula, *et al.*, Phys. Rev. Lett., **98**, 085001 (2007); N. B. Meezan, *et al.*, Phys. Plasmas, **17**, 056304 (2010) X. Meng, *et al.*, Phys. Plasmas, High Power Laser Science and Engineering, **1**, 94 (2012).
- [4] W. L. Kruer, *The physics of laser plasma interactions*, Addison-Wesley, New York (1990).
- [5] H. A. Rose, Phys. Plasmas **2**, 2216 (1995).
- [6] J. Garnier, Phys. Plasmas **6**, 1601 (1999).
- [7] A. A. Vedenov, and L. I. Rudakov, Sov. Phys. Doklady **9**, 1073 (1965); A. M. Rubenchik, Radiophys. Quant. Electron. **17**, 1249 (1976); V. E. Zakharov, S. L. Musher, and A. M. Rubenchik, Phys. Rep. **129**, 285 (1985).
- [8] D. Pesme, *et al.*, Natl. Tech. Inform. Document No. PB92-100312 (1987); arXiv:0710.2195 (2007).
- [9] P. M. Lushnikov and H. A. Rose, Phys. Rev. Lett. **92**, 255003 (2004).
- [10] P. M. Lushnikov and H. A. Rose, Plasma Phys. Controlled Fusion **48**, 1501 (2006).
- [11] H. A. Rose and D. F. DuBois, Phys. Rev. Lett. **72**, 2883 (1994).
- [12] P. M. Lushnikov and H. A. Rose, arXiv:0710.0634 (2007).
- [13] C. Niemann, *et al.*, Phys. Rev. Lett. **100**, 045002 (2008).
- [14] The literature is replete with multi-dimensional simulations of SBS, with models which are similar to the one used in our work (see. e.g. [25–27]). However, the other works emphasize nonlinear regimes with competing instabilities, such as BSBS and filamentation, while we apply our theory and simulation to strictly linear BSBS regime.
- [15] H. A. Rose and Ph. Mounaix, Phys. Plasmas **18**, 042109 (2011).
- [16] A. Bers, pp. 451-517, In *Handbook of plasma physics*, Eds. M.N Rosenbluth, *et al.*, North-Holland (1983).
- [17] L. P. Pitaevskii, and E.M. Lifshitz, *Physical Kinetics: Volume 10*, Butterworth-Heinemann, Oxford (1981).
- [18] Ph. Mounaix, *et al.*, Phys. Rev. Lett. **85**, 4526 (2000).
- [19] D. F. DuBois, B. Bezzerides, and H. A. Rose, Phys. of Fluids B: Plasma Physics **4**, 241 (1992).
- [20] R. H. Lehmburg and S. P. Obenschain, Opt. Commun. **46**, 27 (1983).
- [21] Subsequent analysis can be easily generalized to include polarization smoothing [1].
- [22] H. A. Rose and D. F. DuBois, Phys. of Fluids **B5**, 3337 (1993).
- [23] M.D. Rosen, *et al.*, High Energy Density Physics **7**, 180 (2011).
- [24] This expression is valid for $\mu > \pi/4$, while for $\mu \leq \pi/4$ the convective threshold coincides with the absolute instability threshold.
- [25] A. J. Schmitt and B. B. Afeyan, Phys. Plasmas **5**, 503 (1998).
- [26] P.E. Masson-Laborde, *et al.*, J. De Physique IV **133**, 247 (2006).
- [27] D. Pesme, *et al.*, Phys. Rev. Lett. **84**, 278 (2000); A. V. Maximov, *et al.*, Phys. Plasmas **8**, 1319 (2001); P. Loiseau, *et al.*, Phys. Rev. Lett. **97**, 205001 (2006).